Journal of Geo-Engineering Sciences 1 (2013) 13–36
DOI 10.3233/JGS-130011
IOS Press

Discussion of an instrumented screw pile load test and connected pile group load settlement behavior

P.O. Van Impe[a], W.F. Van Impe[b,*] and L. Seminck[c]
[a]*Visiting Professor University Ghent, Belgium*
[b]*Past-President ISSMGE, Emeritus full professor University Ghent, Belgium*
[c]*CEO of the GFS n.v. industries, Belgium*

Abstract. The aim of the paper is to discuss a fully instrumented screw pile load test up to failure, in difficult heterogeneous soil conditions along the shaft. The pre-stressing of the pile during its installation process has been brought to attention as an important item to assisting in explaining the differences in pile capacity and load settlement curve on the one hand, and the data as registered from the pile shaft instrumentation.

In the second part of the paper, starting info on the registered load settlement data of the foundation slabs of each of the three, closely positioned, oil tanks of 48 m diameter and 19 m of height are shared and briefly analyzed.

Keywords: Screw pile, pile group, residual stress, group effect, pile load testing

1. The oil tanks' foundation engineering problem at the Ostend-Belgium site

1.1. General soil conditions at the site

At the Ostend oil tank site (Fig. 1), the soil conditions, up to depths of roughly 12 to 15 m can be described as very heterogeneous fill (Fig. 2), for the whole area seems to be excavated and hydraulically refilled over decades, before reaching the today's new destination of the site as an oil tank plant.

It means that below some thin or weaker quaternary soil lenses, from about 12–15 m up to depths of about 18 m, the first natural bearing layer would be the tertiary sand (the Tielt formation – "Kortemark" sand package) of about 4 to 5 m thick, only starting from about 18 m on, Fig. 3a,b,c. Below this sand layer a very thick (about 80 to 100 m) tertiary O.C. clay – the "Kortrijk" formation of the Western-Flanders' O.C. clay, is appearing. This clay resembles to some extent the London clay. At the site, the CPT(U) testing unfortunately was not reaching to large depths into this tertiary clay.

The bearing sand layer of about 4 to 5 m thickness does show CPT cone resistances of about 20 Mpa, with peaking resistance over 30 MPa in some cases, while the slightly O.C. clay layer underneath, in the upper part, slowly varies its cone resistance with depth, from about 2.5 to 5 Mpa.

*Corresponding author: W.F. Van Impe, Past-President ISSMGE, Emeritus full professor University Ghent, Belgium. E-mail: William.VanImpe@ugent.be.

ISSN 2213-2880/13/$27.50

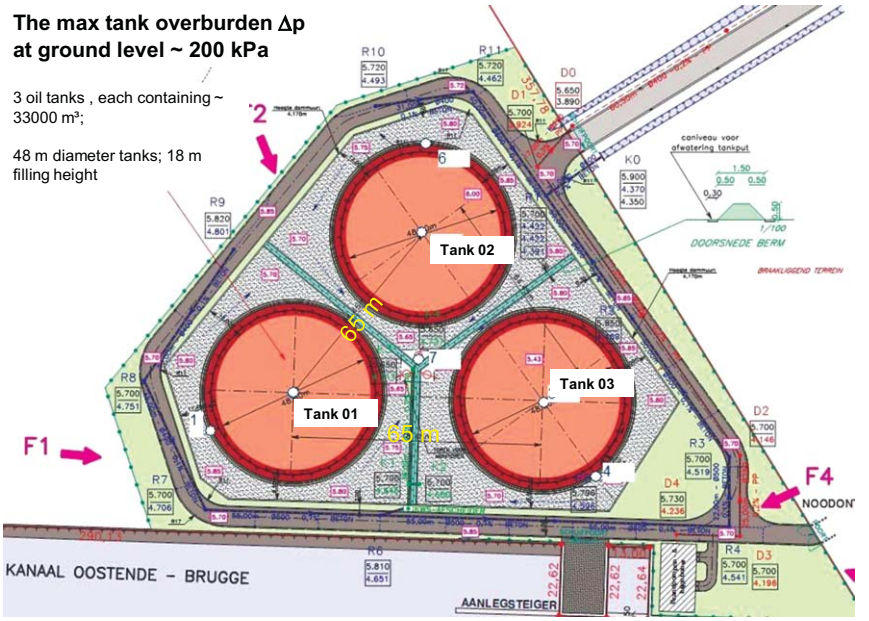

Fig. 1. The site and location of the 3 oil tanks at Ostend – Belgium.

1.2. The oil tank foundation design

The three oil tanks (Fig. 1) each containing 33000 m^3 are steel structures of 48 m in diameter, and 19 m high, positioned in a triangular shape at a center to center inter-distance of 65 m from each other. The foundation slab under each tank, covering some 422 displacement cast in situ screw piles as the tank's bearing pile group, is conceived as a 0.60 m thick reinforced foundation slab of some 49 m diameter. The 460 mm diameter (method [1, 2]) displacement screw piles of the Omega pile type (Fig. 4) at an inter-distance of 2.2 m axis to axis, are designed to take each a maximum design load of 960 kN, including some 180 kN negative skin friction load, all with an global safety of about 2. The actual unit overburden load of a fully loaded tank with foundation slab is indeed rising up to about 220 kN/m^2, determining a total foundation load still to be increased by some negative skin friction loading. Such negative skin friction up to at most 17 m depth, originates from the reconsolidation of the soft layers along the pile shaft, as a result of the remolding by the pile group installation itself.

The conclusion is that the foundation design of the oil tanks can actually be considered as a foundation on a large group of 400 end bearing displacement screw piles, cast in situ, until about 22 m of depth. The ultimate pile tip capacity (about 1750 kN), at the optimum pile tip level, can be increased with the ultimate pile shaft capacity in the about 3.5 m bearing sand layer situated above the pile tip (about 200 kN), to reach a full total ultimate pile capacity of about 1950 kN and so the allowable capacity of >960 kN.

2. Instrumented single pile test load

2.1. Ground conditions at the test pile location

In order to optimize the design method, a fully (extensometer) instrumented test pile was installed (Fig. 6a and b) to be test loaded up to a pile base settlement of 10% of the pile base diameter; which in accordance to the Belgian practice is corresponding to the required deformation at "failure load" of a soil displacement pile.

The ground conditions at the (21.56 m long) test pile axis location is given in Fig. 5a, b; at the site the ground water table can be assumed at about 0.5 m below natural ground level.

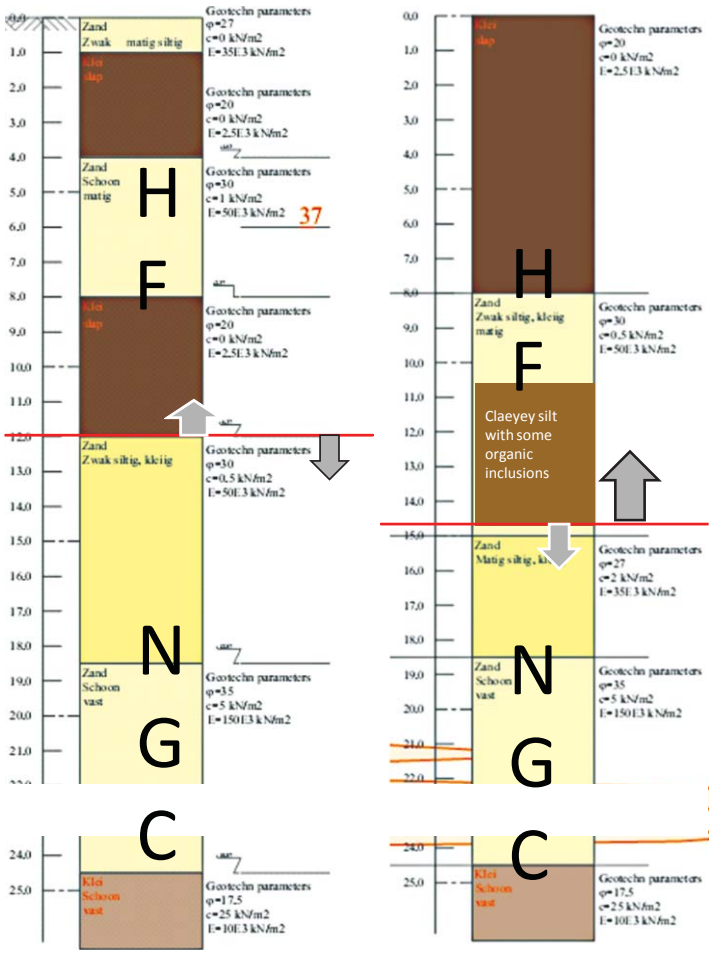

Fig. 2. General overview of typical bore profiling outcome at the oil tank site (HF = hydraullc fill; NG = quaternary and tertairy natural ground layers).

The pile base is anchored in the tertiairy dense sand layer, overlying the tertiairy slightly O.C. 100 m thick clay formation, starting from about 2.5 m ($>5\Phi_{pile}$) below the pile tip; the 6 extensometers are located at the depths shown in Fig. 5b.

2.2. *Prediction of the pile capacity according an adapted Belgian method*

The unit ultimate pile base (460 mm diameter) capacity (method Van Impe-De Beer- 1986) [1, 2], times the pile base area, (cfr Fig. 6c and d), increased by the ultimate pile shaft capacity on the lower part of the pile shaft mainly, has been applied in order to predict the total ultimate pile capacity of the test pile. The result of this ultimate total pile capacity (Qult) prediction, linked to the CPT result at the location of the test pile is shown in Fig. 7.

At the test pile base level (21.56 m depth) such capacity prediction would consequently lead to a values of: total ultimate pile tip capacity of 2168 kN; total ultimate shaft capacity of 1943 kN. This results in a total ultimate pile capacity of Qult $\sim$ 4.1 MN. The above mentioned pile shaft capacity prediction, from CPT, in this case however should be interpreted cautiously, since the pile installation itself in this type of soil heterogeneous fill material is highly sensitive to reconsolidation and so even to negative skin friction effects. It means that the upper 11 m of the shaft capacity contribution in accordance with this CPT result is highly questionable and should not be taken into account.

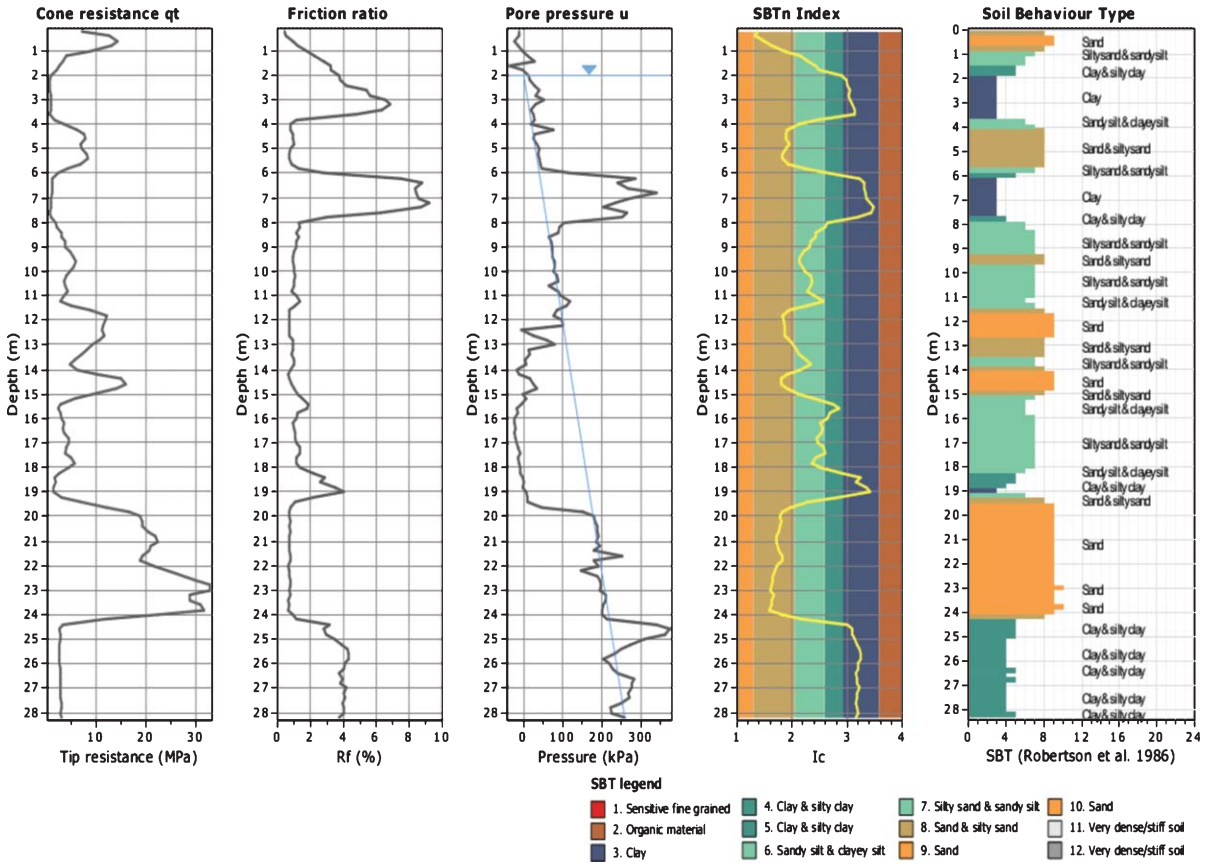

Fig. 3a. Characteristic CPTU result at the site of the oil tanks in Ostend [3, 4].

The only reliable positive shaft capacity contribution one can count on would be the capacity from the layer in between 11 m and 21 m depth, above the pile tip. This would in our opinion finally lead to an adapted total ultimate pile capacity Qult of 2168 kN + 1400 kN ~ 3500 kN.

2.3. the estimated stiffness moduli relevant to the pile test load

The casted concrete quality (C30/37), including the pile reinforcement cage and the extensometercage as instrumentation of the test pile, was bringing us at an estimate of the test pile concrete stiffness of Ec = 32000 MPa. The test pile concrete block on top (from level −046 m to + 1.04 m) would have a stiffness of 30 GPa.

The stiffness values estimated for the various soil layers identified (cfr Fig. 5b) along the pile shaft and underneath the pile tip at the test pile location, are summarized in Table 1.

The predicted pile load-settlement curve (Van Impe W.F. -1986, 1994) – Fig. 8, using the above mentioned stiffness estimates and the failure criterion of Qult at 10% pile tip settlement, would bring us to a value of about 3350 kN.

2.4. Measured load-settlement data of the test pile and corresponding capacity discussion

The actual test pile stiffness evaluation was performed on the basis of the [5] proposal of plotting $\Delta\sigma/\Delta\ \varepsilon$ at the locations of each of the extensometers in the pile shaft, versus the local strain ε at that respective locations. Figure 9 is showing these results. All curves measured during the pile load test seem to more or less converge at values of

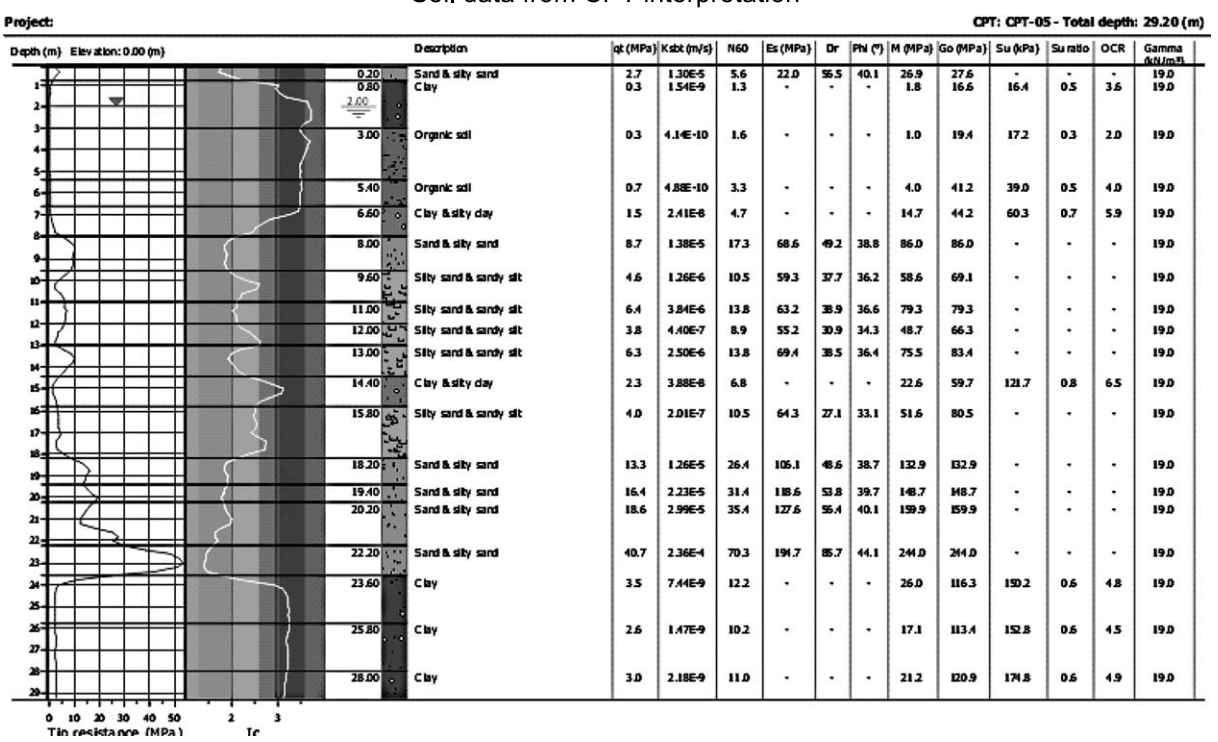

Fig. 3b. Example of soil data estimation from CPT interpretation at the site adapted [5, 6].

$\Delta\sigma/\Delta\ \varepsilon$ of 6, corresponding to a pile stiffness of about 30 GPa; which is not so far from the first estimate we made at the start of the pile installation (32 GPa [3, 4]).

Starting from the pile stiffness evaluated now from the pile test, we can draw the load distribution in the pile at the extensometer locations for the increasing pile head load levels during the load testing of the pile. The Fig. 10a,b are showing the measured data interpreted in this way. From the measured data (cfr Fig. 10) one could read that the large deformations (>46 mm = 10% of the pile tip diameter) of the pile tip, with subsequent ongoing pile tip displacements do appear at pile head load levels in between 3300 kN and 3600 kN. This is fairly well corresponding to the CPT- predicted "failure" load of about 3.5 MN, and to the from predicted load-settlement curve ultimate load of 3.35 MN, all mentioned above.

One has to remind that all of such predictions do start from the assumption of a perfect pile soil interaction corresponding to the assumed installation factors implemented in the design method (cfr Fig. 6c).

Even with the ultimate test pile load corresponding quite well to the predicted values, the distribution of the ultimate pile tip load versus the ultimate pile shaft load as measured appears to be quite different from the predicted distribution, discussed above under 2.2. The expected shaft capacity to be developed starting from the CPT results at the test pile location, as compared to the measured values during the test loading of the pile is indicated in Fig. 11.

The rather low tip bearing capacity mobilized during the pile test load can be partly explained by the indeed too weak soil- pile tip interaction at the base, caused by the long reinforcement cage with inner extensometer cage, both fitting only narrowly inside the rather small diameter opening left open by the re-screwed auger head during the casting of the concrete. The concrete flow in such case is not satisfying the requirements for a good soil-pile tip interaction. In the standard screw pile execution of this type of pile, the reinforcement cage is never reaching the pile tip level, and obviously there is no supplementary cage for the instrumentation.

The typical S-shaped load-distribution curve, and so the connected over-estimation of the unit pile shaft friction in the upper layers, is a result of induced residual strains (and stresses) in the pile due to installation procedures

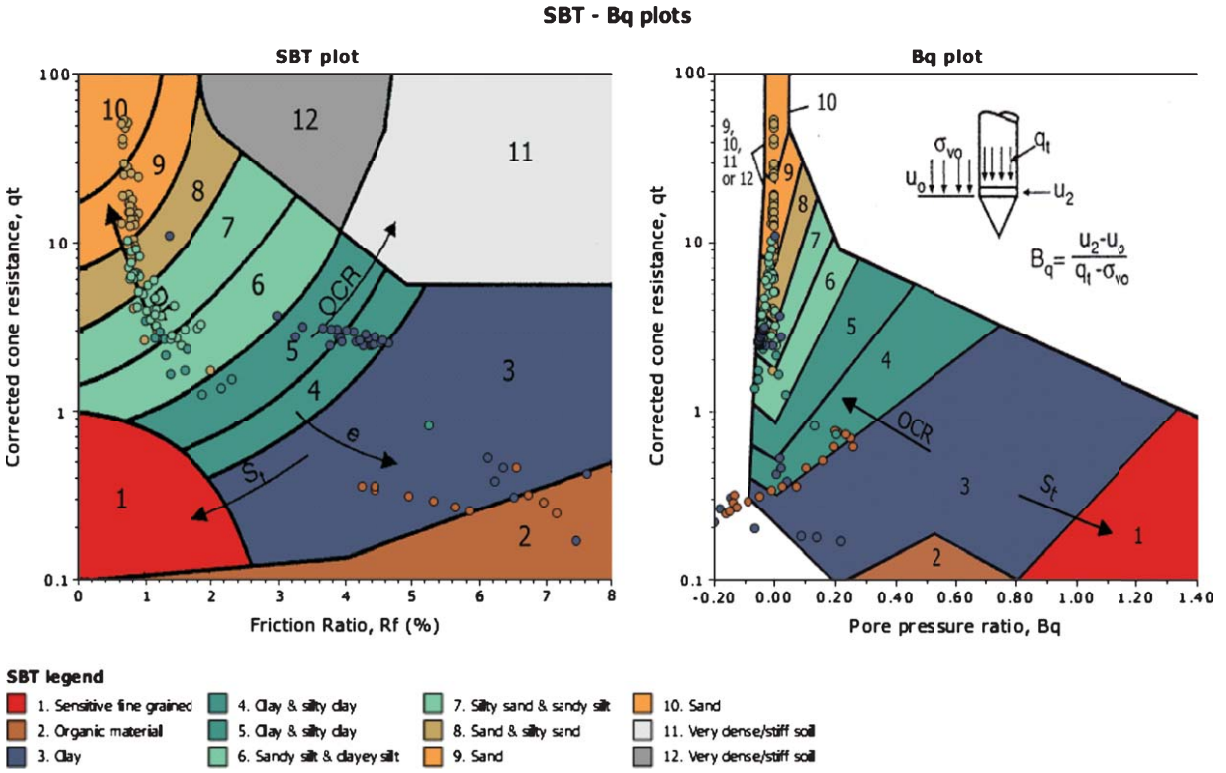

Fig. 3c. Soil layers classif. (P. Robertson -1986 method) from all CPT(U) at the Ostend oil tank site [3, 4].

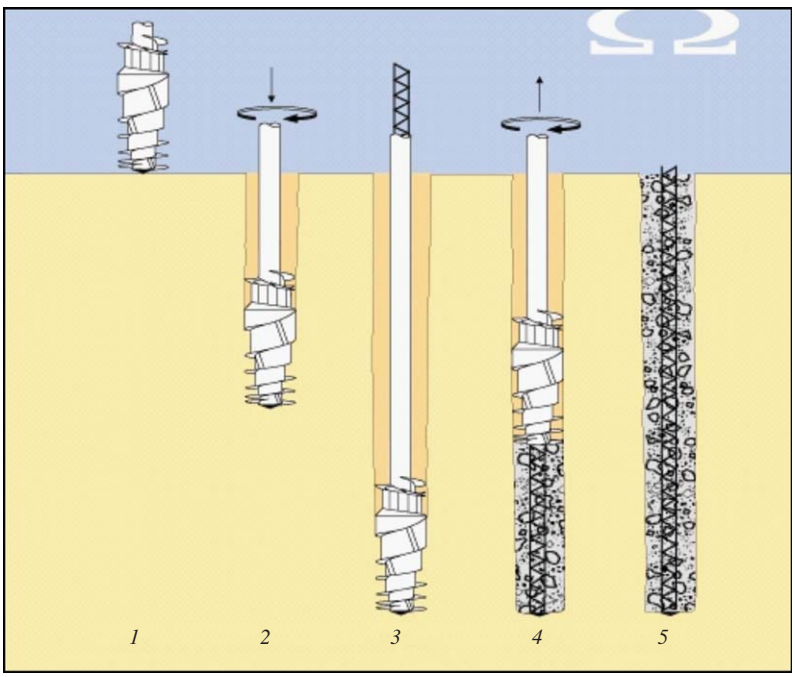

Fig. 4. The Omega screw pile type in Belgium [1, 2].

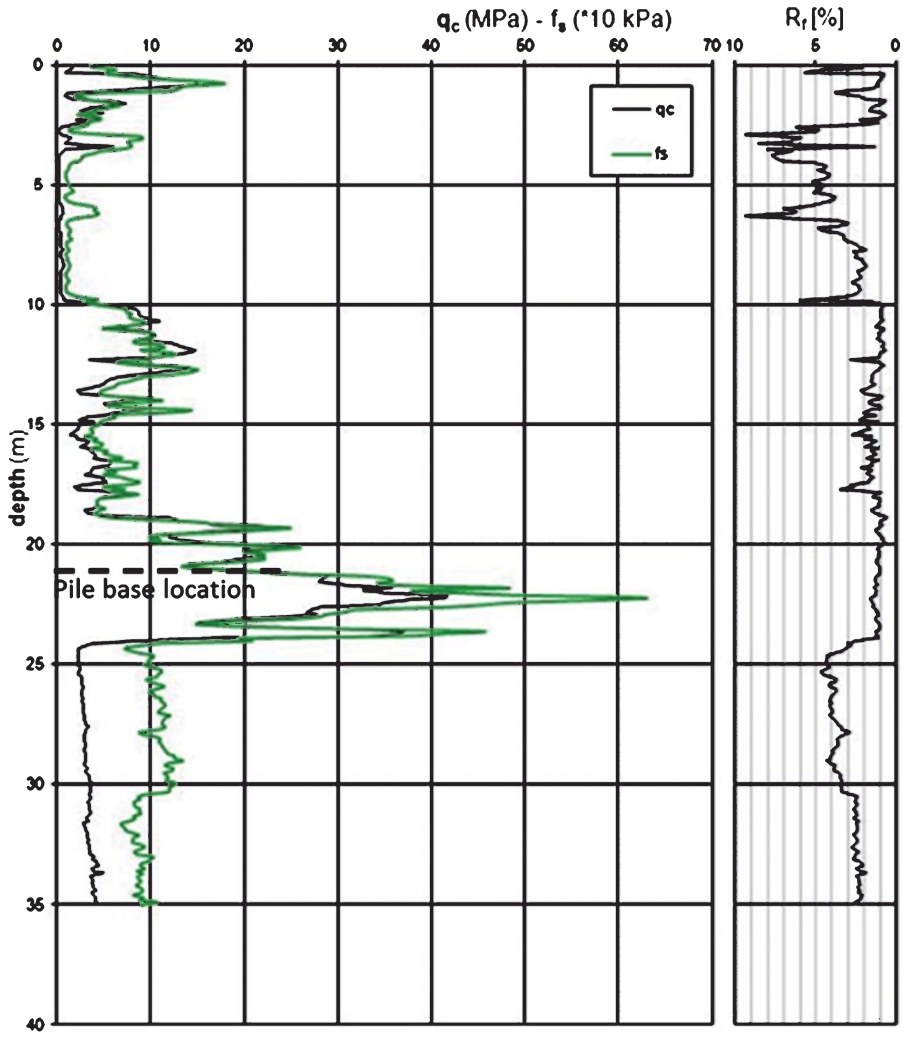

Fig. 5a. CPT result at the location of the test pile axis; pile base at 21.56 m depth.

in the specific soil conditions (cfr also [6]). The zero readings of the instrumentation in the pile, after the residual strains were developed, do obviously influence the interpretation of the load-settlement curves of a pile assumed to start from zero initial stress levels at zero pile head loading. The residual loads indeed quite present here, could be linked to the reconsolidation, due to pile installation effects, of the softer layers (from 4 m till 10 m depth, and from 14.7 m till 17 m depth) and consequently resulting from the negative skin friction mobilized in the entire soil layer in between 1 m and 17 m depth.

The Fig. 12 indicates with the full blue line, the test pile load distribution during the test loading at a level of 3005 kN pile head load (of the assumed not pre-stressed pile). The green dashed line indicates the negative skin friction developed along the pile shaft due to reconsolidation of the soil layer in between 1 m and 17 m depth. This is, consequently, the new zero-reference line for the extensometer readings. The actual, corrected pile load distribution curve therefore would be the full green line in Fig. 12, reflecting indeed the much higher pile tip load contribution and the expected ratio pile shaft to pile tip load as one would derive from the CPT-based or the rational load-settlement curve based predictions, and leading to a pile base load of about 1.7 MN at a pile head load of 3 MN; so with a shaft load contribution of 1.3 MN.

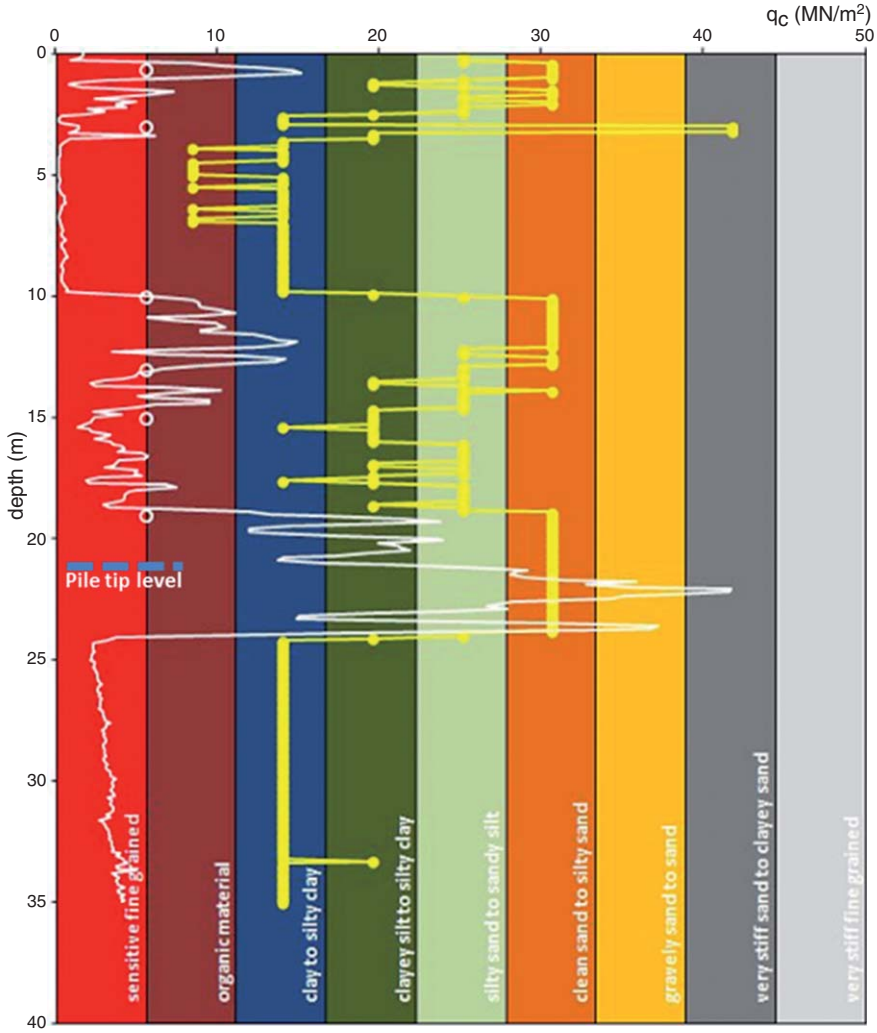

Fig. 5b. CPT based (qc: white line) soil type classification (yellow lines- [3] method), at the location of the test pile axis. White (o) are the extensometer locations in the test pile.

Table 1
Estimated stiffness parameters, from the CPT result at the test pile location

Depth (m)	qc (Mpa)	E (Mpa)	M (Mpa)	G0 (Mpa)
0,66	4,60	34	40	45
3	0,66	4	5	23
10	10,07	77	97	97
14,5	5,28	63	66	80
18	15,80	118	143	147
21,56	35,68	225	282	282
22,48	26,18	170	209	214
24	3,3	27	27	114
35	5,23	51	51	156

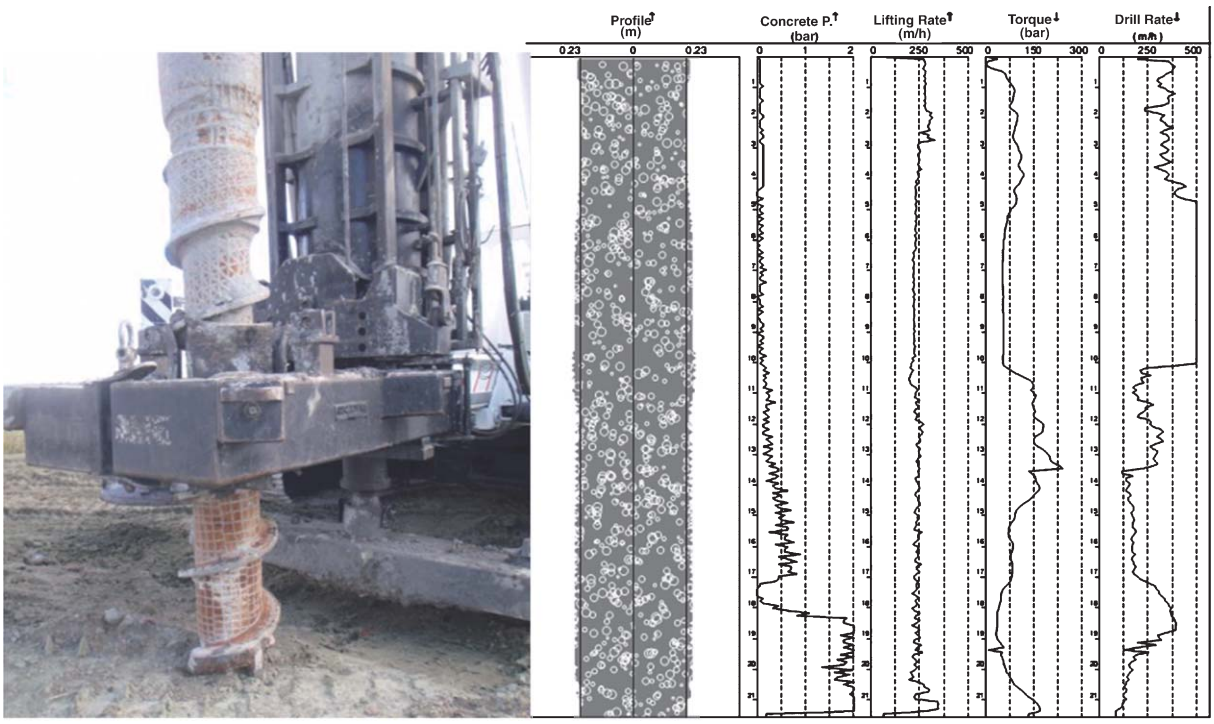

Fig. 6a. Test pile installation parameters of the test pile, instrumented on the reinforcement cage at 6 depth locations.

The dashed green line is calculated starting from the assumption of a perfect soil-pile tip interaction, which is not necessarily the case for this instrumented test pile, as argued before. So, the dotted lines in Fig. 12 do suggest other possible shape developments of the dashed green curve, including some influence of a less perfect soil- pile tip interaction. The most reliable correction of this type in our opinion is the correction shown by the dotted line from level −17 m on. This would lead to a tip load of about 1.2 MN at a pile head load of 3 MN; so with a shaft load contribution of 1.8 MN.

Only the from lab testing derived stiffness of the soil underneath the already installed pile tip, would lead to more reliable outcome of the pile tip interaction stiffness required to optimize the interpretation of the load-distribution curve measured during the pile load test. Without this our theoretical modeling cannot be calibrated to the pile load test outcome as such, because the unknown parameters, already mentioned, in the equation still prohibit a unique solution of the inverse problem to solve.

But, the outcome of this pile load test is anyhow showing clearly that the total ultimate pile load is – even with safety factors over $F > 3$ – satisfying largely the design load and also confirms that the expected load settlement stiffness at design load satisfies the criterion of pile tip deformations of about 3 mm at 1.5 times the design load.

The ratio of the pile shaft to pile tip mobilization at ultimate capacity loading level seems to be about 0.65 to 0.7, from the corrected test results, corresponding quite well with all CPT based predictions.

2.5. Load-settlement data of the test pile and corresponding pile group deformation discussion

A very simple approach of evaluation safely the expected pile group settlements from the unique pile load-settlement behavior and with the stiffness parameters safely evaluated from the CPT test results, as for example done for the test pile in Table 1, would be to go out from an “equivalent raft” principle. In our case of a clearly end bearing pile group of 422 piles, diameter 460 mm, at 2.2 m inter distance each; loaded at the top level with a

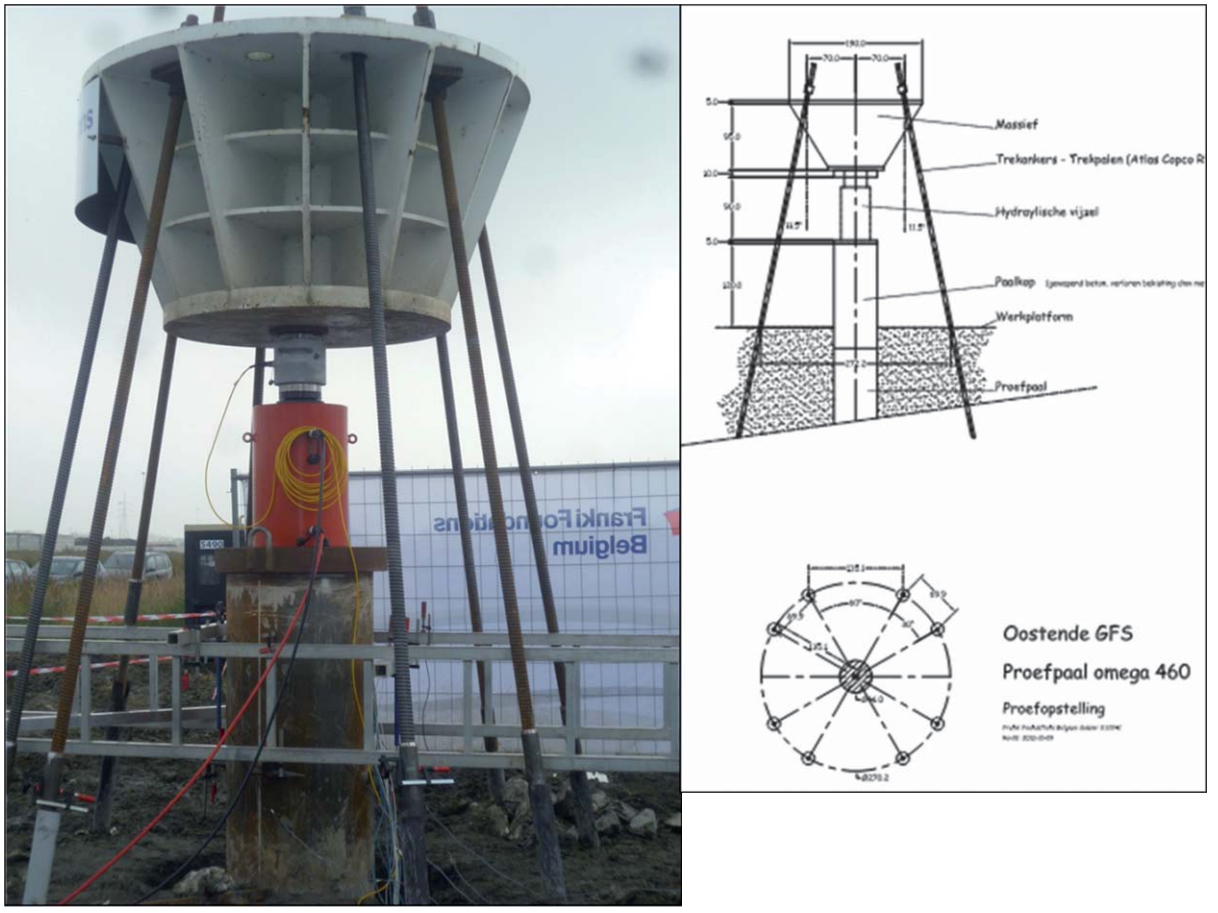

Fig. 6b. Test pile loading system, with 8 deep anchors inclined at 12°, each enabling a 500 kN tensile force.

full hydro-tested 33000 m³ oil tank of 48 m diameter and the 0.6 m thick concrete top plate; i.e; with about Δp at foundation top level of the pile group of 200 kPa (Fig. 13).

The equivalent fully end bearing pile group equivalent raft, installed here in this case at 18.16 m depth, with an equivalent outspreaded diameter of 54.29 m, under an equivalent Δp unit load at that depth of 170 kPa, would give us a safe estimate of an upper level of the overall elastic oil tank deformation of 27 mm, to be increased by an upper level of the soil plastic deformations of about 110 mm, due to the consolidation effects of the relevant interfering layers into the foundation engineering problem. We went out for this elastic deformation estimate of the pile group, from the stiffness interaction between pile tip and soil as we could derive from the pile test loading. It's however expected that the piles at the locations of the oil tanks – having no reinforcement cage up to the pile base nor a cage for pile instrumentation - would show a stiffer pile base-soil interaction. This would bring down the expected pile group deformations. In addition, the in reality expected elastic deformations during the very short time hydro-test (it takes at most a 4 days full load) at tank loading, in our views should be lower. All the above together, the deformations during the hydro testing therefore can be expected to become for example of the order of about 70% of the previous elastic longer term values.

The mentioned lasting plastic deformations due to consolidation effects are much more difficult to judge, since we don't have enough consolidation parameter information measured in the lab of the 100 m thick tertiary clay underneath the tank foundation sand layer at the tank location (Fig. 14a,b). In addition the interaction of the 3 tanks' loading, since they are only at 65 m axis-to-axis inter-distance, leads unavoidably to a settlement trough as we even during the hydro testing already could notice to some extent.

Ultimate base resistance

$$R_{bu} = \beta.\alpha_b.\varepsilon_b.q_{bu}^{(m)}.A_b = \beta.\alpha_b.\varepsilon_b.Q_{bu}$$

β = 1,0

α_b = pile installation factor = 0.7 here for this pile type

ε_b = parameter for stiff clays

$q_{bu}^{(m)}$ or $q_{r,b}$ = ultimate **unit** pile base resistance

(Van Impe/ De Beer method -1986) ⟶

A_b = nominal pile base cross section area

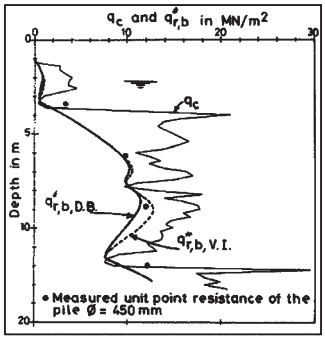

Ultimate shaft resistance

$$R_{su} = \xi_f.X_s.\sum H_i.q_{sui} = \xi_f.X_s.\sum H_i.\eta_p^{*}q_{ci}$$

ξ_f = pile installation factor = 1.0

η_p^{*} = soil parameter, here in the tertiairy dense sand : 1/ 150

q_{ci} = cone resistance at the considered depth i

Hi = the pile shaft height corresponding to the considered layer i

Xs = the pile shaft perimeter

Fig. 6c. The ultimate pile capacity, from CPT testing - the Belgian approach.

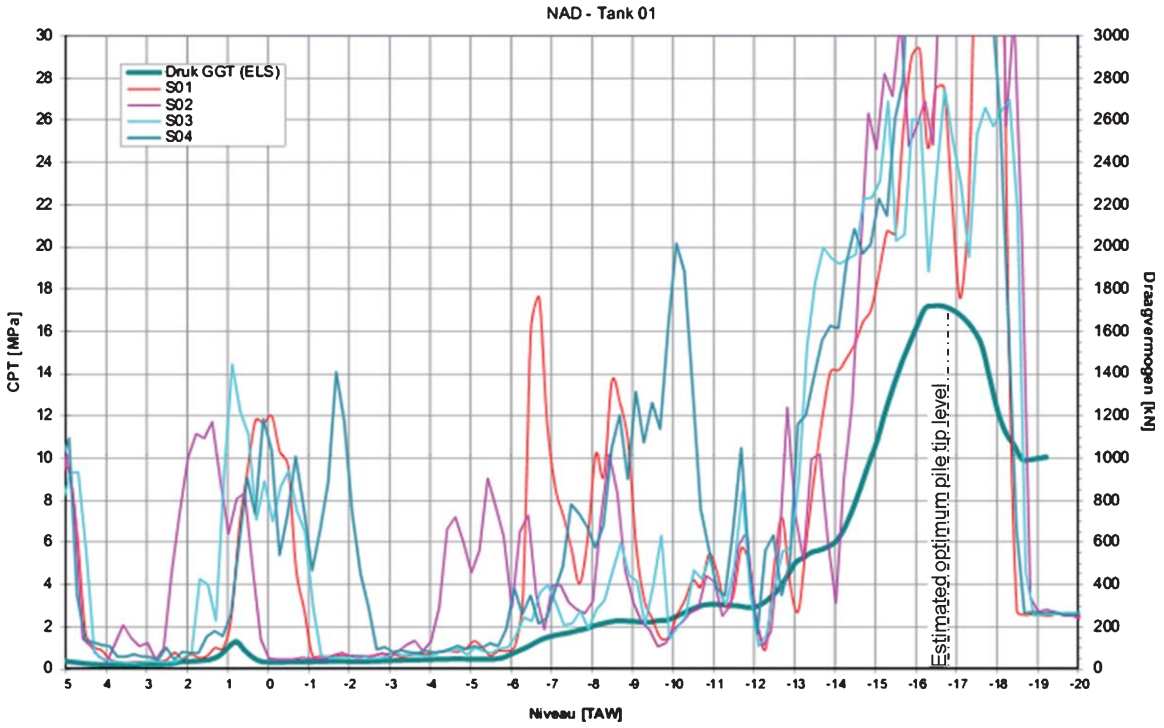

Fig. 6d. Examples of typical CPT-results in the tank(01) area and its derived total ultimate pile tip capacity at corresponding levels of possible pile tip depths method [1, 2].

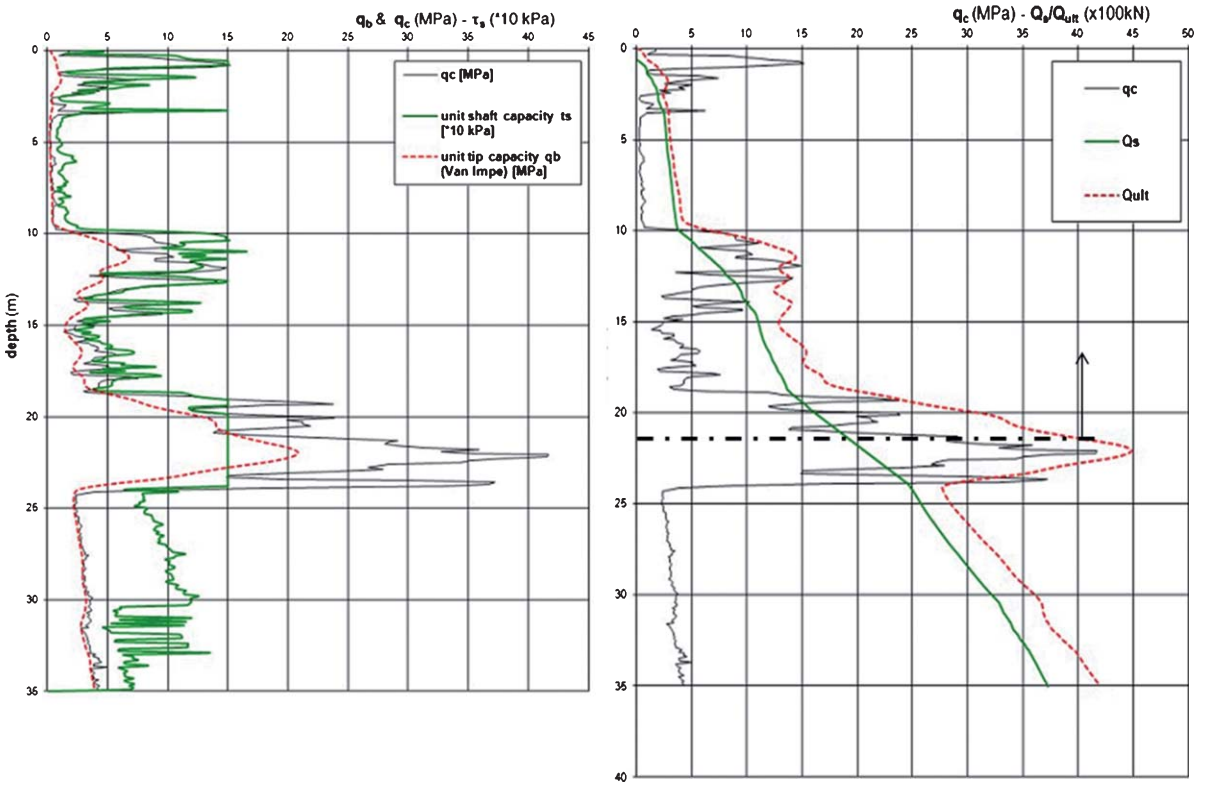

Fig. 7. The unit pile tip and unit pile shaft values; the total Ultimate pile capacity Quıt with depth at the location of the axis of the test pile [1, 2].

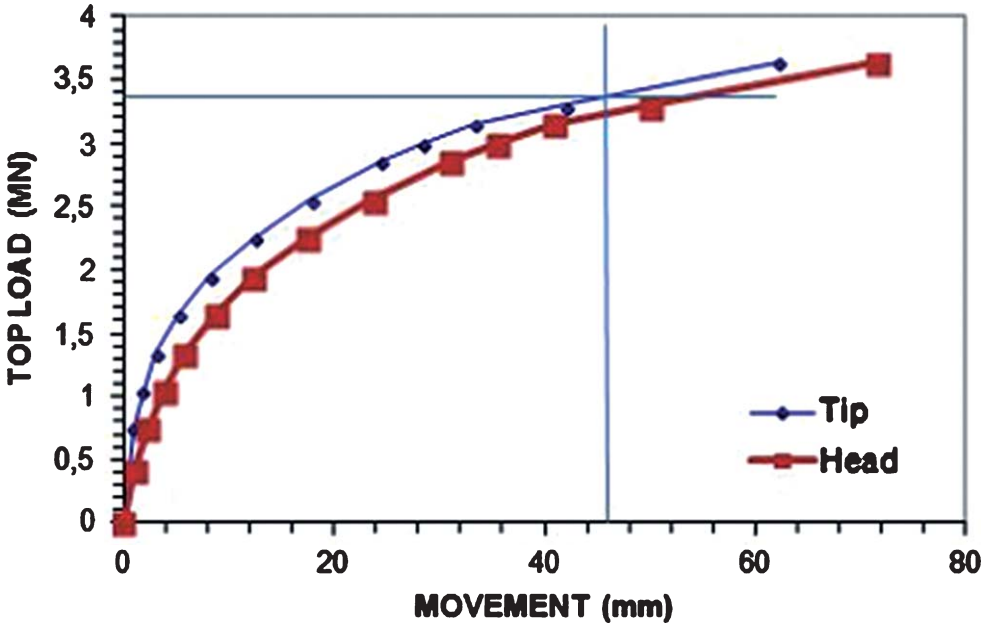

Fig. 8. Estimated total ultimate pile capacity from the predicted pile load-settlement curve (Van Impe W.F. 1986–1994) [1, 2].

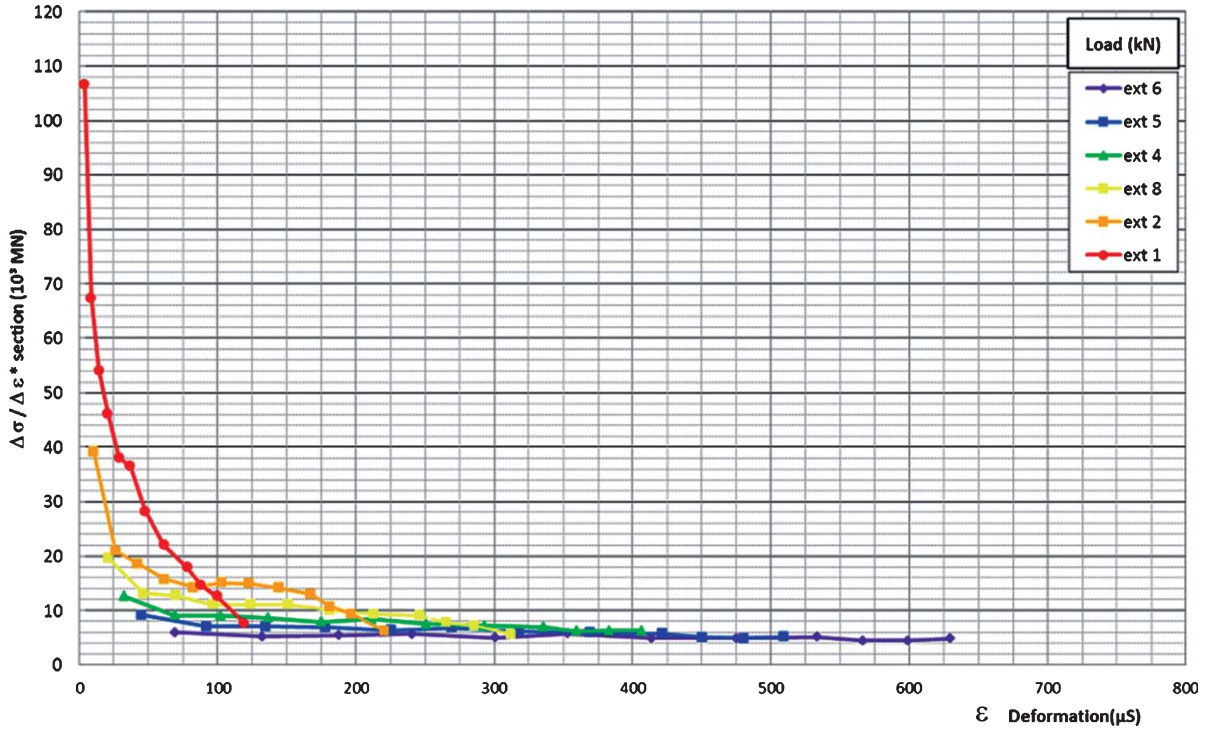

Fig. 9. (Fellenius 2001 method) stiffness evaluation of the test pile with best fit for all extensometers [5, 6].

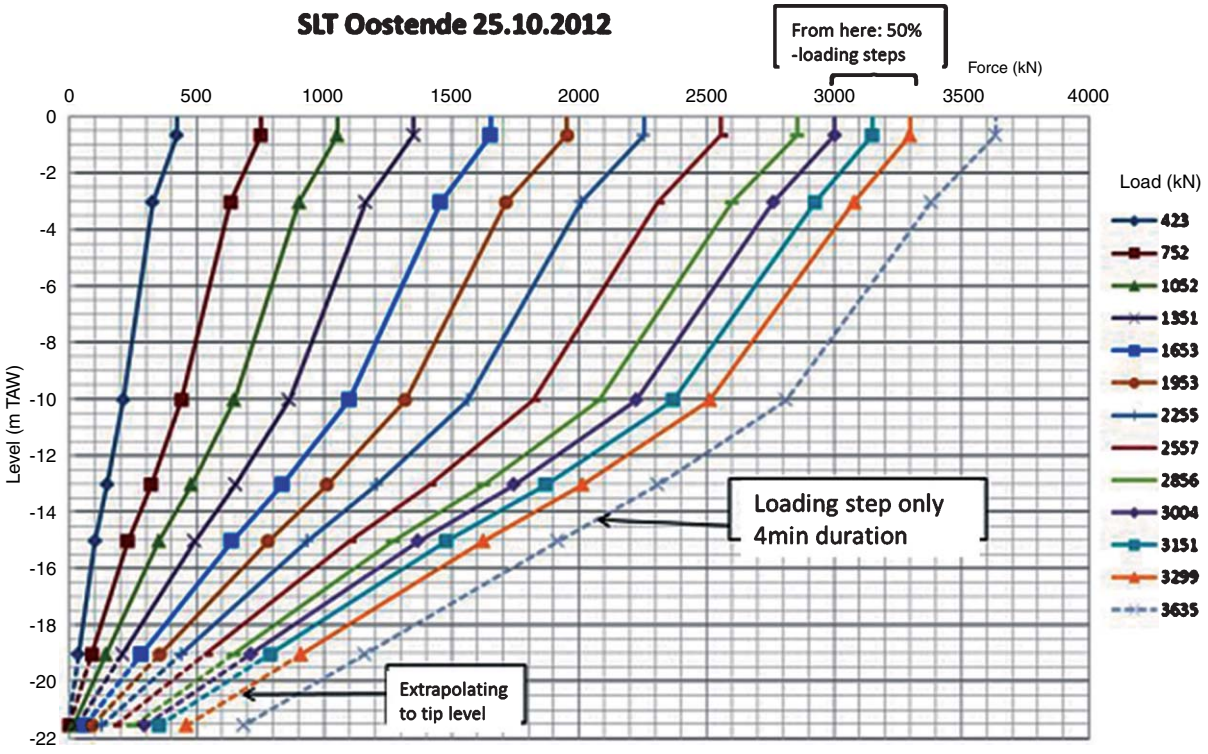

Fig. 10a. Axial load distribution in the test pile at the extensometer levels, and extrapolated to the pile base level.

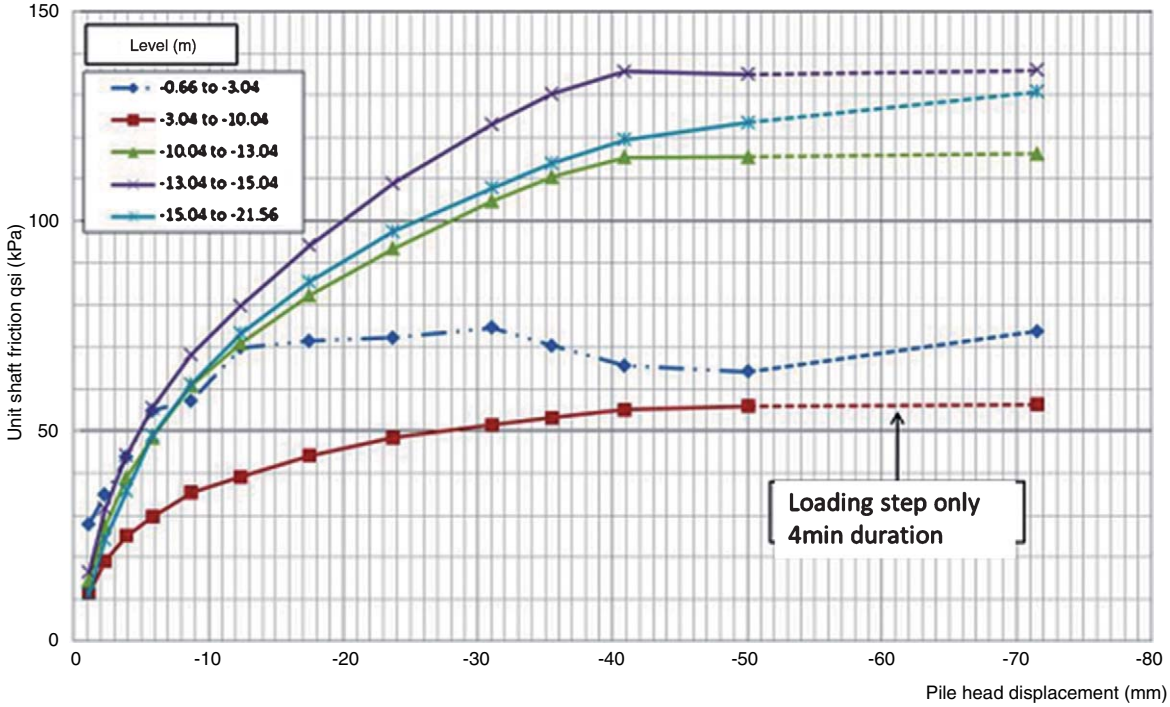

Fig. 10b. Mobilising the pile shaft capacity at increasing pile deformations, in the sections in between the expensometer levels.

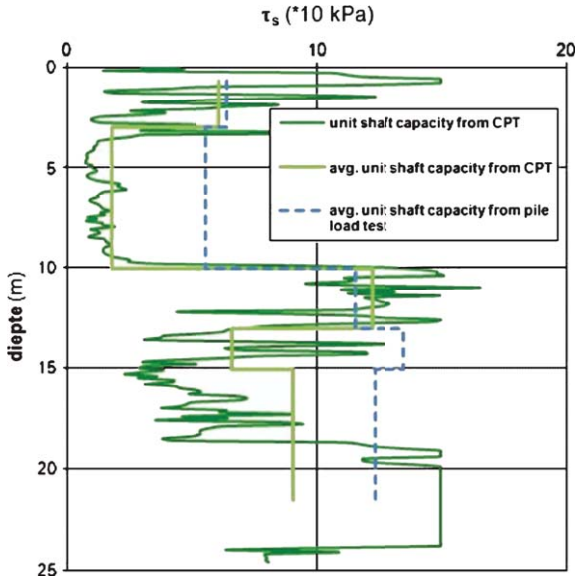

Fig. 11. Comparison of the mobilised unit shaft friction along the test pile shaft; CPT based predicted mobilised friction versus the measured values during the laod test.

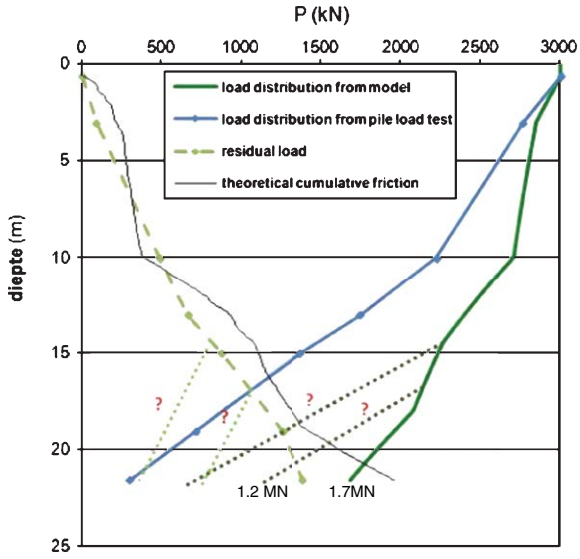

Fig. 12. Corrected test pile laod distribution implementing the residual stress induced loading.

Fig. 13. Tanks nr 01 and 02, at the end of construction.

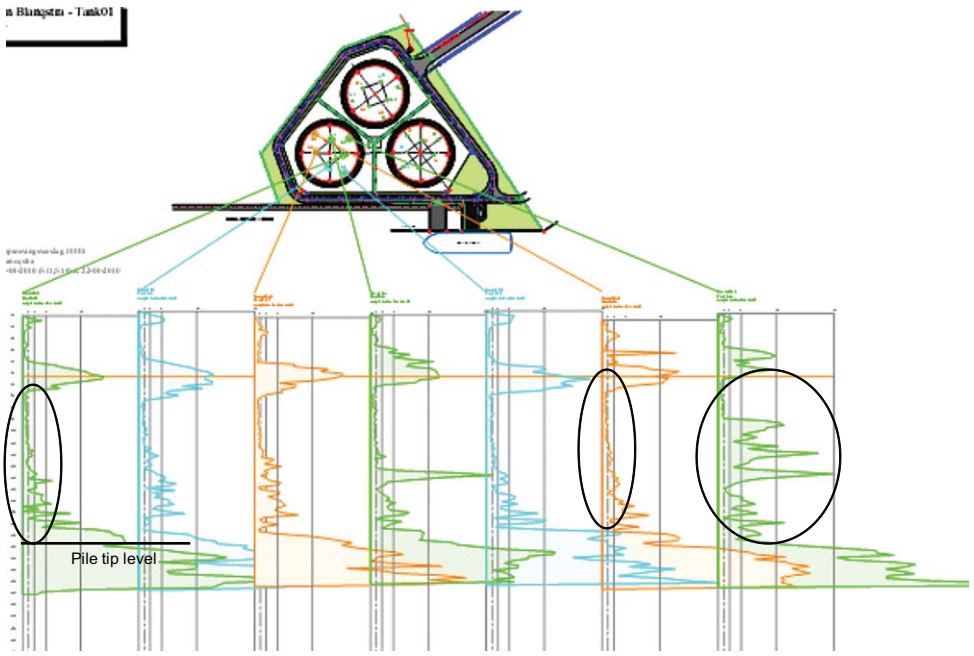

Fig. 14a. Pattern of CPT-soil resistance variability under the tank 01.

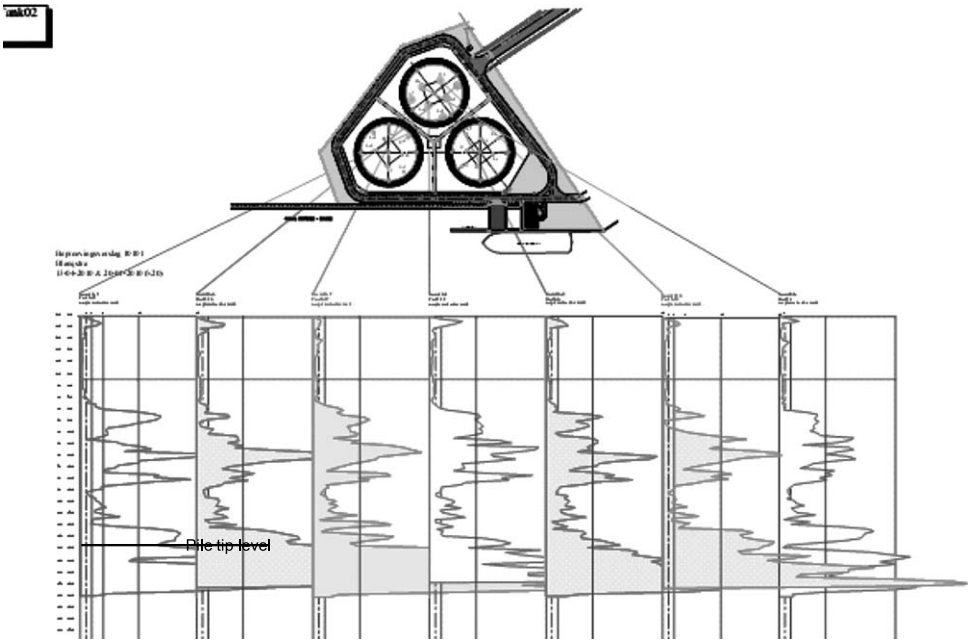

Fig. 14b. Pattern of soil resistance variability under the tank 02.

3. The tanks' foundation pile group settlement, from the hydro – load testing

3.1. Hydro-test loading and data measurement procedures

The hydro-testing of the 3 tanks was performed in April 2013. All tanks were filled, subsequently, with water to a height of about 18 m; the filling of one tank taking about 3 days of time. The water level in the tanks was kept constant afterwards for about 4 days, followed by the emptying procedure of the tanks in a period of 3 days again. Tank nr 01 was first in the water filling procedure, followed, with a certain overlap in time by tank 02; concluding, after emptying tank 02 by the filling of tank 03. The history of this loading pattern as well as the measured mean settlements are indicated in Fig. 15.

A series of 16 measurements points equally divided at an center angle of 22.5° from each other, along the foundation slab perimeter of a tank, are used to follow closely each movement of the foundation slab of each of the tanks.

The data gathered during the hydro-testing of the 3 tanks are summarized in Tables 2, 3 and 4.

At each loading step in time of a tank, the average overall settlement, the deviation from the average settlement of each of the 16 perimeter points, the planar tilt of the best fitting plane, as well as the out-of-plane settlement of each of the 16 perimeter points and the out-of-plane deflection of each point, leading to a measure for the curvature of the tank wall at the level of the foundation slab.

In Fig. 16 the full load-settlement curves at the loading/unloading during the hydro testing of each of the tanks has been reproduced; as from the data of the Tables 2, 3 and 4. The reference mark for the settlements of tank 01 very unfortunately moved unnoticed, vertically over about 5 mm during the load testing. It means that the green curve on the Fig. 16 at its full load should probably be situated around a settlement range of 15 mm (green dashed line on the figure).

The mean overall tank "immediate" settlement during the short period of hydro testing apparently is of the order of 20 mm; with some 5 to 6 mmm remaining average settlement after total unloading of the tanks. The loading of the tank fillings not reaching even the 200 kPa, assumed in our predicted elastic settlements, it can be stated that the measured short time elastic settlement values do fit quite well our expectations at this site.

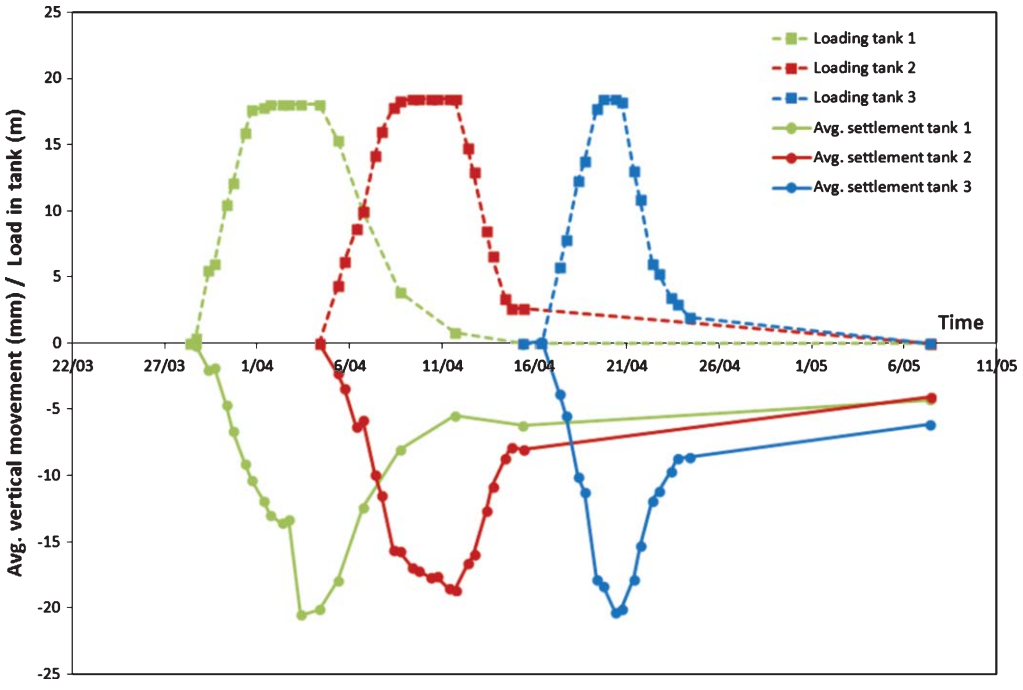

Fig. 15. Tanks' water loading history and measured vertical displacements.

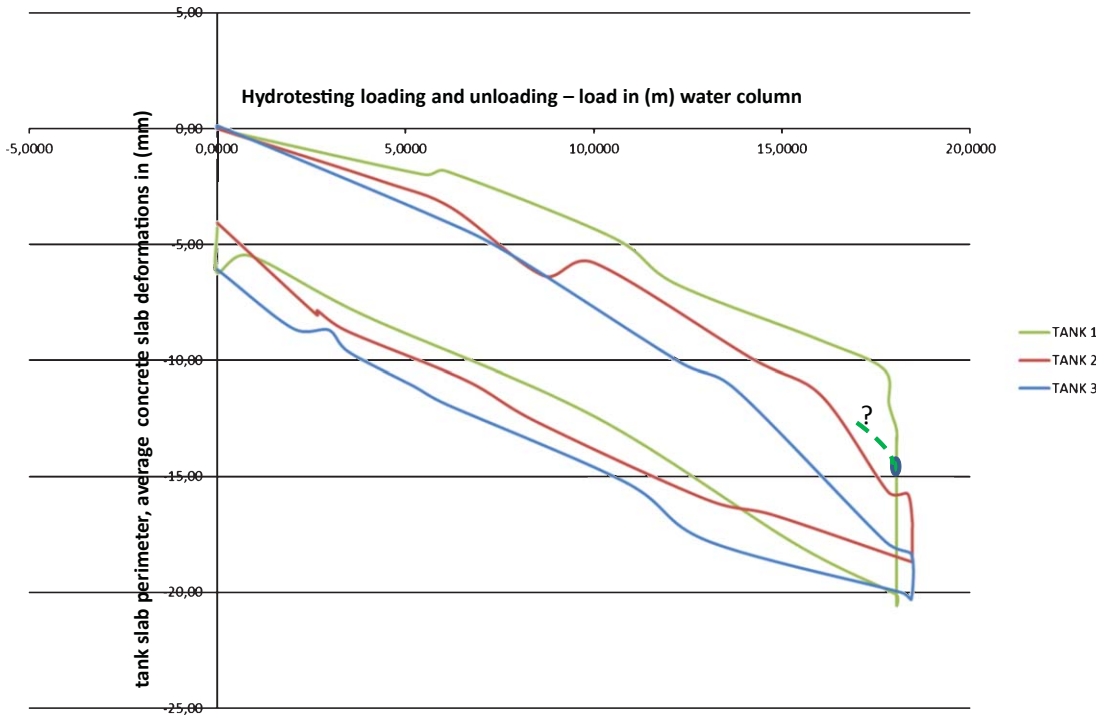

Fig. 16. The full load-settlement curves for each of the oil tanks at hydro – testing with unloading.

The rotation or tilting of the foundation slab during the hydro loading tests on the tanks has been summarized – from the Tables 2, 3 and 4 data – for the major loading conditions, in the Fig. 17.

The first conclusion can be that after all, all tank foundation slab tilting values do remain very low; as such not more than 3 to 4 mm over a tank diameter of 48 m; so a rotation of as low as <1/12000.

The tank 01 is almost not tilting at all in the loading stage (A line not differing a lot from the A line in Fig. 17a). Some increasing of the tilting is shown at the unloading stage (line B), but all disappears more or less in the final unloaded stage (line C). the rotation of the tank 01 in the unloading stage is clearly oriented towards the center of the 3 tanks' locations, tank 02 being loaded during the unloading stage of tank 01 (cfr Fig. 15).

Tank 02 is tilting is clearly influenced by the interaction of the loading schemes in tanks 01 and 02. The reference line of the zero tank 02 slab condition (line 0 in Fig. 17b) was measured at the time (4th of April in the afternoon) of full loading of tank 01. The unloaded foundation slab plain of tank 02 therefore was already tilting 04 mm towards the tank 01 at the start of the filling of tank 02. It means that the tilting shown in Fig. 17b (lines A,B and C) all start from an inclined plain towards tank 01. So, the downward tilt of –3 mm of perimeter point 3 at full loading conditions of tank 02, is no more than a back tilting of the initial upheave the foundation slab plain had at that point 3 due to the tank 01 influence. Similarly, the upward tilting of perimeter point 11 by some 1.8 mm at full loading of the tank 02 is induced by the back tilting of the entire foundation slab from the initial condition influenced by tank 01. The remaining tilt of tank 02, (line C) in this respect is reflecting a more or less horizontal tank slab after full unloading, when interpreting the data on lines A, B and C with the initial tilting of the slab plain.

The foundation slab of Tank 03 had much less initial tilting(reference line 0) due to the influence of the tanks 01 and 02; the soil conditions at the location of tank 03 being rather different form the rest of the tank site. The initial tilting towards tank 01 of the foundation slab was not more than about 1 mm. It means that the 0 –line in the Fig. 17c is indicating a slightly tilted foundation slab of tank 03 towards tank 01; at the start of its filling (tanks 01 and 02 being already empty at that moment – cfr Fig. 15). The remaining tilt (line C) after full unloading of the tank 03 therefore (cfr Fig. 17c) is higher than for the tanks 01 and 02; but after all not more than about 2.5 mm towards

Table 2

Perimeter top of concrete slab measuring: tank 01

	H = fill hight of the water at corresponding date and time; shown as /(8)a.m. or at /(4)p.m.																			empty tank
Measured	H	0,00 m	0,45 m	5,50 m	6,06 m	10,50 m	12,15 m	15,95 m	17,69 m	17,84 m	18,04 m	18,04 m	18,04 m	18,04 m	18,04 m	15,36 m	10,00 m	3,89 m	0,84 m	0,00 m	0,00 m
Points	time	28-03/(8)	28-03/(4)	29-03/(8)	29-03/(4)	30-03/(8)	30-03/(4)	31-03/(8)	31-03/(4)	01-04/(8)	01-04/(4)	02-04/(8)	02-04/(4)	03-04/(8)	04-04/(8)	05-04/(8)	06-04/(4)	08-04/(4)	11-04/(4)	15-04/(8)	07-05/(8)
B101		0	−0.1	−2.08	−1.58	−4.22	−6.83	−8.56	−10.48	−11.43	−12.92	−13.11	−12.4	−20.22	−20.11	−18.15	−12.8	−9.31	−6.94	−6.5	−4.2
B102		0	−0.48	−2.28	−1.77	−4.41	−6.94	−9.13	−10.59	−11.81	−13.31	−13.62	−12.92	−20.3	−20.48	−18.4	−13.09	−10.71	−8.34	−6.93	−4.58
B103		0	−0.14	−2.29	−2.11	−4.76	−7.22	−9.38	−11.12	−12.29	−13.83	−14.26	−13.15	−21.24	−19.28	−19.19	−15.26	−10.83	−8.48	−7.13	−4.44
B104		0	−0.19	−2.33	−1.56	−4.72	−6.28	−9.04	−10.29	−11.46	−12.06	−13.02	−12.39	−20.5	−20.15	−18.59	−14.32	−9.85	−7.32	−6.57	−4.16
B105		0	−0.25	−2.01	−2.24	−5.5	−6.85	−9.47	−10.55	−12.59	−13.15	−14.31	−15.06	−21.55	−21.36	−18.8	−13.42	−9.63	−6.78	−7.15	−4.26
B106		0	−0.29	−1.8	−1.66	−5.15	−6.78	−8.95	−10.08	−11.78	−12.13	−13.59	−14.05	−20.29	−20.49	−17.48	−12.07	−8.01	−5.41	−6.25	−3.73
B107		0	−0.06	−1.92	−1.75	−5.26	−7.15	−9.77	−10.96	−13.07	−13.59	−14.79	−15.09	−21.66	−21.65	−18.96	−12.58	−7.79	−5.48	−6.71	−4.76
B108		0	−0.13	−1.88	−1.71	−4.96	−6.54	−9.27	−10.55	−12.43	−13	−13.77	−14.24	−20.94	−20.81	−18.19	−11.84	−7.03	−4.3	−6.08	−4.48
B109		0	−0.32	−1.89	−2	−4.99	−6.62	−9.12	−10.15	−12.04	−12.85	−13.86	−13.79	−20.19	−20.01	−17.48	−11.57	−6.85	−4	−5.56	−3.92
B110		0	−0.19	−1.82	−1.73	−4.96	−6.39	−9.35	−10.61	−12.34	−13.15	−13.99	−13.78	−20.86	−20.17	−17.34	−12.25	−6.89	−4.28	−5.82	−4.01
B111		0	−0.11	−1.75	−1.79	−4.81	−6.54	−9.15	−10.38	−11.95	−12.94	−13.81	−13.48	−20.54	−19.87	−17.88	−11.49	−6.72	−4.01	−5.78	−4.3
B112		0	−0.17	−1.86	−1.83	−4.11	−6.25	−8.77	−9.9	−11.39	−12.52	−12.83	−12.46	−19.75	−19.38	−16.98	−10.82	−6.12	−3.54	−5.27	−3.93
B113		0	−0.22	−1.97	−1.87	−4.15	−6.48	−8.87	−9.69	−11.22	−12.72	−13.08	−12.38	−20.08	−19.5	−16.82	−11.05	−6.24	−3.75	−5.64	−3.98
B114		0	−0.08	−1.96	−1.69	−4.42	−6.55	−8.94	−9.9	−11.32	−12.87	−13.08	−12.45	−20.02	−18.37	−16.43	−11.37	−6.63	−4.23	−5.75	−4.25
B115		0	−0.21	−1.99	−2.09	−4.64	−6.57	−8.85	−10.19	−11.43	−13.23	−13.31	−12.95	−20.1	−19.92	−17.61	−11.91	−7.69	−4.97	−6.01	−4.49
B116		0	0.05	−1.87	−1.78	−4.05	−6.82	−8.78	−10.31	−11.7	−13.17	−13.14	−12.45	−20.31	−20.14	−18.31	−12.38	−8.49	−5.81	−6.43	−4.88

Increasing level differences of the 16 perimeter measuring points, in mm.

Table 3

Perimeter top of concrete slab measuring: tank 02

		H = fill hight of the water at corresponding date and time, shown as /(8)a.m. or /(4)p.m.																					empty tank
Measured	H	0,00 m	4,40 m	6,20 m	8,67 m	10,00 m	14,19 m	16,03 m	17,82 m	18,33 m	18,46 m	18,46 m	18,46 m	18,46 m	18,46 m	18,46 m	14,77 m	12,98 m	8,50 m	6,61 m	3,42 m	2,65 m	2,65 m	0,00 m
Points	time	04-04/(8)	05-04/(8)	05-04/(4)	06-04/(8)	06-04/(4)	07-04/(8)	07-04/(4)	08-04/(8)	08-04/(4)	09-04/(8)	09-04/(4)	10-04/(8)	10-04/(4)	11-04/(8)	11-04/(4)	12-04/(8)	12-04/(4)	13-04/(8)	13-04/(4)	14-04/(8)	14-04/(4)	15-04/(8)	07-05 /(8)
B201		0	−2.22	−2.88	−6.23	−5.68	−9.87	−11.51	−15.38	−15.77	−17.1	−17.06	−17.99	−17.97	−18.5	−19.02	−16.52	−16.15	−13.07	−11.17	−9.24	−8.41	−7.86	−4.92
B202		0	−3.27	−4.17	−7.76	−6.77	−11.93	−13.8	−17.63	−17.26	−18.34	−19.43	−19.86	−19.58	−20.62	−21.53	−19.4	−18.55	−15.39	−12.7	−10.84	−10.46	−9.65	−5.78
B203		0	−2.77	−4.07	−7.36	−6.68	−11.63	−13.62	−17.98	−18.07	−19.42	−19.84	−20.56	−20.67	−21.43	−21.58	−19.81	−18.53	−15.29	−13.78	−11.43	−10.36	−10.79	−6.86
B204		0	−1.88	−3.47	−6.51	−6.31	−10.62	−12.49	−16.32	−16.46	−18.16	−17.7	−18.92	−19.1	−19.95	−20.03	−17.23	−17.15	−13.9	−12.48	−10.1	−9.15	−9.39	−3.96
B205		0	−1.84	−3	−6.17	−5.79	−9.89	−11.88	−15.78	−16.07	−17.4	−17.69	−18.12	−18.35	−19.08	−19.25	−17.42	−16.59	−13.12	−11.7	−9.47	−8.46	−8.69	−4.59
B206		0	−1.77	−2.88	−5.83	−5.85	−9.69	−11.58	−15.54	−15.78	−17.25	−17.59	−17.82	−18.02	−18.91	−19.15	−17.19	−16.22	−12.93	−11.95	−9.09	−8.16	−8.89	−4.15
B207		0	−2.24	−3.29	−6.07	−5.95	−10.37	−11.41	−16.23	−16.41	−17.6	−17.97	−18.35	−17.91	−19.51	−19.37	−17.38	−16.64	−13.07	−11.35	−9.18	−8.14	−8.58	−4.54
B208		0	−2.28	−3.76	−6.36	−6.13	−10.23	−11.15	−15.83	−15.71	−16.87	−17.41	−17.6	−17.07	−18.73	−18.38	−16.69	−15.88	−12.62	−10.78	−8.66	−7.66	−8.2	−3.85
B209		0	−2.04	−3.36	−5.47	−5.46	−9.2	−9.97	−14.33	−14.52	−15.5	−15.78	−15.99	−15.51	−17.04	−16.75	−15.08	−14.18	−10.92	−9.13	−7.22	−6.31	−6.43	−2.35
B210		0	−2.2	−3.39	−5.78	−4.71	−8.89	−10.06	−14.27	−14.3	−15.43	−15.55	−15.63	−15.67	−16.69	−16.63	−14.73	−14.37	−10.69	−8.54	−5.78	−5.91	−6.05	−2.11
B211		0	−2.05	−3.41	−5.75	−4.6	−8.96	−10.47	−14.73	−14.63	−15.58	−15.78	−16.09	−16.08	−16.75	−16.97	−14.88	−14.22	−10.67	−8.74	−6.73	−5.59	−6	−1.97
B212		0	−1.98	−3.3	−5.51	−4.91	−8.64	−10.48	−14.61	−14.66	−15.49	−15.55	−16.14	−16.05	−16.88	−16.93	−14.92	−14.27	−10.93	−9.43	−7.21	−6.31	−6.61	−2.59
B213		0	−1.94	−3.12	−5.46	−4.97	−8.82	−10.5	−14.58	−14.76	−15.84	−15.92	−16.4	−16.45	−17.2	−17.4	−15.26	−14.51	−11.25	−9.69	−7.71	−6.69	−6.94	−3.32
B214		0	−2.3	−3.22	−8.09	−5.28	−9.42	−10.61	−14.73	−14.72	−16.07	−16.29	−16.44	−16.86	−17.44	−17.62	−15.65	−15.04	−11.72	−9.78	−8	−6.88	−7.27	−4
B215		0	−2.92	−3.66	−6.67	−7.74	−10.3	−12.14	−16.27	−16.32	−17.82	−18.08	−18.36	−18.54	−19.04	−19.22	−17.23	−16.63	−13.34	−11.43	−9.38	−8.34	−8.62	−5.07
B216		0	−2.84	−3.38	−6.61	−5.74	−10.15	−12.16	−16.44	−16.27	−17.49	−17.85	−18.57	−18.62	−19.03	−19.19	−17.17	−16.73	−13.5	−11.06	−9.44	−8.67	−8.81	−5.04

Increasing level differences of the 16 perimeter measuring points, in mm.

Table 4

Perimeter top of concrete slab measuring: tank 03

		H = fill hight of the water at corresponding date and time, shown as /(8)a.m. or /(4)p.m															empty tank
Measured	H	0.00 m	5,80 m	7,80 m	12,28 m	13,76 m	17,76 m	18,43 m	18,43 m	18,19 m	13,03 m	10,84 m	6,04 m	5,25 m	3,49 m	2,96 m	2,00 m	0.00 m
Points	time	16-04/(8)	17-04/(8)	17-04/(4)	18-04/(8)	18-04 (4)	19-04/(8)	19-04/(4)	20-04/(8)	20-04/(4)	21-04/(8)	21-04/(4)	22-04/(8)	22-04/(4)	23-04/(8)	23-04/(4)	24-04/(8)	07-05/(8)
B301		0.2	−3.69	−5.35	−10.4	−10.84	−17.34	−17.73	−19.89	−18.41	−16.73	−13.34	−10.21	−9.71	−9.08	−7.94	−7.6	−4.94
B302		−0.05	−3.84	−5.6	−10.08	−11.27	−17.57	−17.9	−20.04	−19.49	−17.1	−14.34	−11.1	−10.26	−9.69	−8.09	−8.25	−5.32
B303		0.18	−4.14	−5.46	−9.93	−10.19	−16.93	−17.38	−19.21	−18.63	−16.63	−13.31	−10.78	−10.63	−9.76	−8.24	−8.09	−5.57
B304		−0.06	−4.27	−5.22	−9.91	−10.28	−17.3	−17.76	−19.82	−19.47	−17.47	−14.51	−11.23	−10.92	−9.52	−8.07	−8.33	−6.07
B305		0.05	−4.08	−5.45	−10.08	−10.16	−17.4	−18.05	−19.59	−19.78	−17.88	−14	−11.05	−10.77	−7.68	−7.66	−8.5	−6.09
B306		0.34	−4.15	−5.45	−10.54	−10.57	−18.05	−18.68	−21.14	−20.71	−18.66	−15.2	−11.87	−11.09	−10.08	−8.74	−9.01	−6.47
B307		0.04	−4.15	−5.46	−10.78	−10.67	−17.86	−18.67	−21.07	−20.72	−18.4	−15.3	−12.27	−11.69	−10.4	−9.18	−9.58	−7.31
B308		0.18	−3.73	−5.08	−10.06	−10.85	−18.36	−18.51	−20.8	−20.31	−18.57	−15.27	−12.31	−11.88	−10.49	−8.84	−9.39	−6.89
B309		0	−4.67	−6.51	−11.19	−12	−18.78	−18.93	−19.13	−21.17	−19.08	−16.23	−13.89	−13.74	−10.33	−10.57	−9.49	−8.26
B310		0.46	−3.13	−4.89	−9.45	−11.56	−17.68	−18.52	−20.82	−20.86	−17.42	−15.43	−12.34	−11.25	−9.76	−7.32	−8.71	−6.37
B311		0.56	−3.59	−5.13	−9.73	−12.25	−18.16	−18.96	−20.88	−20.1	−17.95	−15.64	−12.35	−11.13	−9.96	−9.37	−8.76	−5.94
B312		0.04	−4.07	−5.67	−10.48	−12.99	−19.17	−20.32	−22.25	−21.5	−19.53	−16.99	−13.53	−12.49	−11.2	−10.59	−9.86	−7.00
B313		0.03	−3.84	−5.57	−10.22	−12.83	−18.92	−19.75	−21.64	−21.31	−19.07	−16.22	−13.37	−12	−10.73	−10.02	−9.51	−6.54
B314		0.31	−3.62	−5.19	−9.78	−12.24	−18.06	−18.51	−20.53	−20.63	−17.67	−15.15	−12.34	−11.7	−10.08	−9.47	−8.85	−6.07
B315		0.16	−3.45	−5.14	−9.61	−10.43	−16.77	−16.86	−19.04	−18.86	−16.12	−19.62	−10.78	−9.61	−7.74	−7.68	−7.46	−4.90
B316		−0.37	−2.68	−5.81	−8.86	−10.58	−16.93	−16.89	−19.13	−18.31	−16.23	−13.38	−10.14	−9.22	−7.71	−7.26	−6.47	−3.53

Increasing level differences of the 16 perimeter measuring points, in mm.

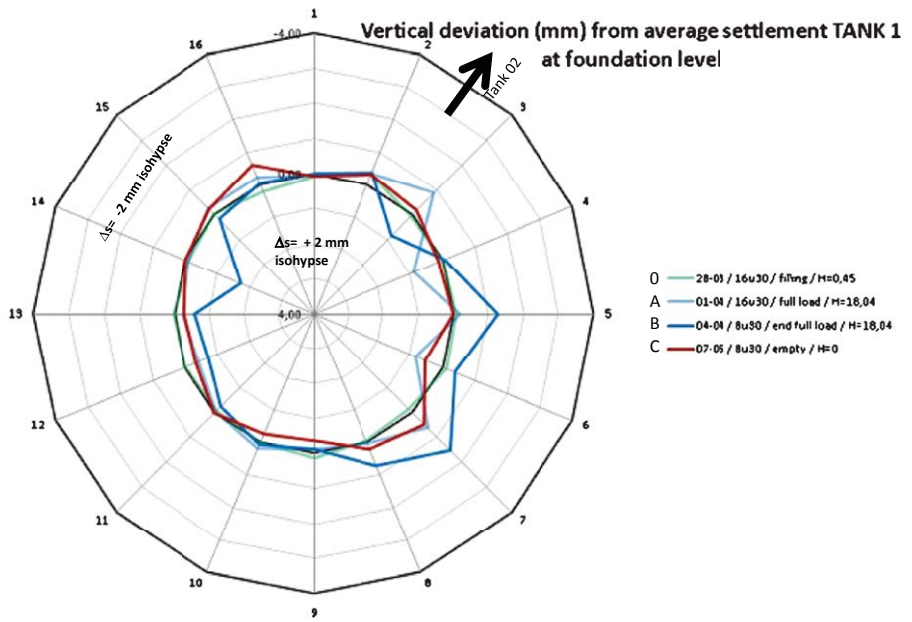

Fig. 17a. Measured deformations of tank 01 conrete slab foundation - during hydrotest (Tanks 02 and 03 still empty).

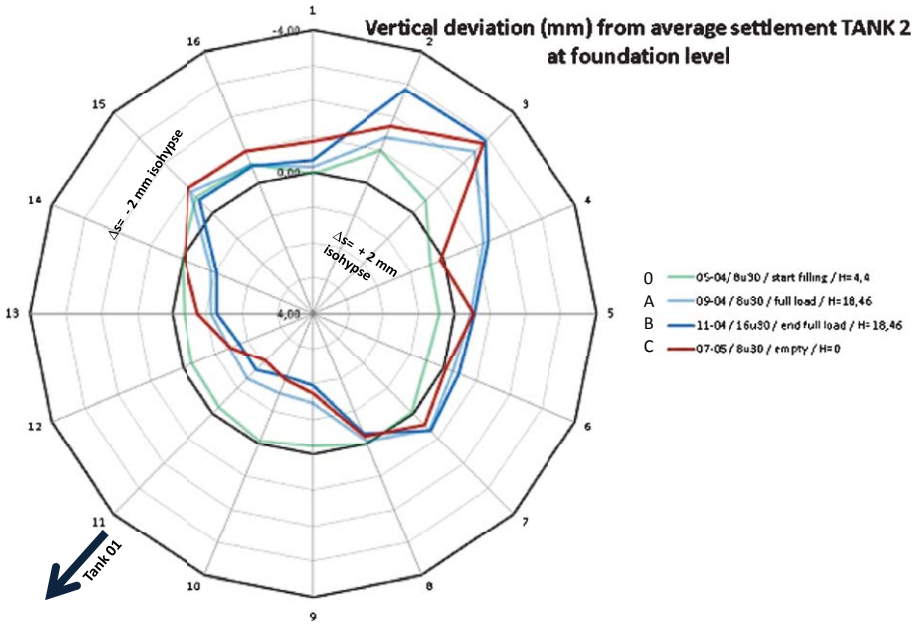

Fig. 17b. Measured deformations of tank 02 conrete slab foundation - during hydrotest.

the South. This can again be attributed to the much more heterogeneous soil conditions at this location; it means quite variable stiffness distributions in the foundation soil.

Another summarizing figure of this tilting process and measured data is gathered in Fig. 18, indicating the direction and the cycles of the tilting movement from the measured data, for each of the tanks in hydro-test loading conditions.

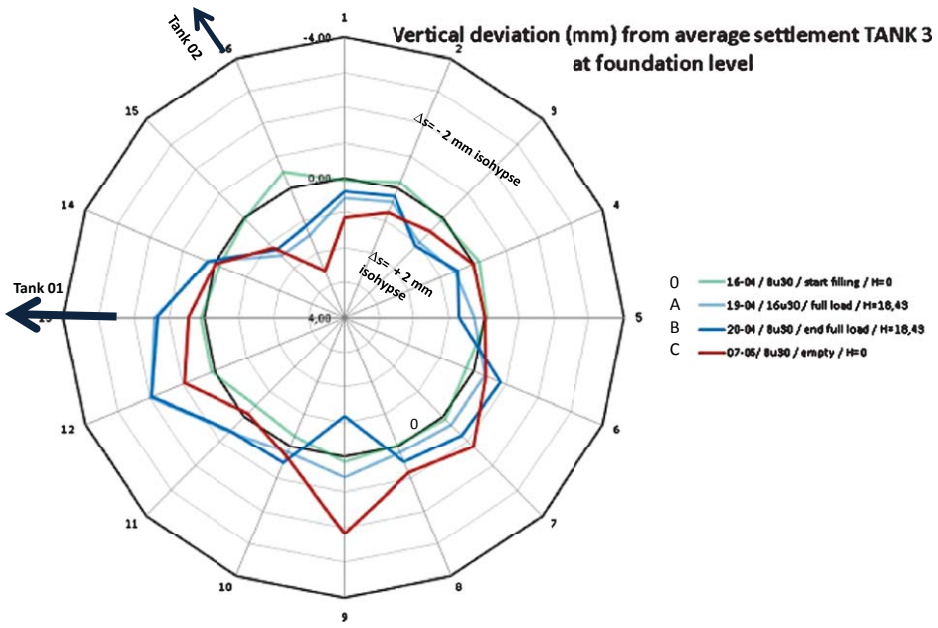

Fig. 17c. Measured deformations of tank 03 conrete slab foundation - during hydrotest.

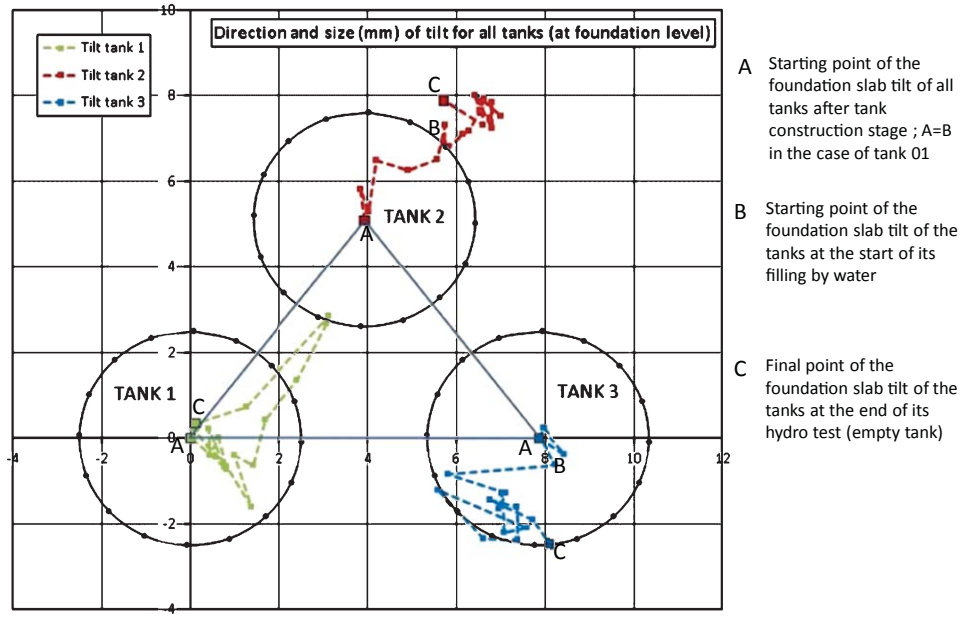

Fig. 18. Cycle of tilting movement and remaining tilt for each of the 3 tanks during hydro-testing.

4. Conclusions

The load-settlement analysis of the pile group measured data, in prediction based on the instrumented single pile load test up to "failure", are showing the usefull potential of such simple prediction methods quite well. The data of the hydro tested oil tanks do illustrate that the end bearing displacement screw pile group underneath each 3 of

the tanks, although in an almost 18 m very heterogeneous soil layering, can guarantee the quite uniform settlement of each of the tanks to a very similar level, governed by the stiffness of the bearing sand layer and the thick slightly OC clay layer underneath. At loading level somewhat less than 200 kPa, the overall settlement range is of the order of 20 mm in the hydro-test elastic settlement period of time. The long term consolidation governed settlements are for the moment evaluated up to more than 110 mm, but are still to be verified by the consolidation characteristics of the thick OC clay layer.

The tilting history of each of the foundation slabs underneath the hydro-tested tanks are indicating that the tilt is never exceeding more than 4 mm in the foundation plain with a radius of 48 m; and that a settlement trough starts to develop by the mutual interaction of the 3 tanks at short distance from each other. Such very small deformation differences from one side of a tank diameter to the other, are fully irrelevant to the tank structure as such, since such deformations are easily absorbed by the 50 mm sand asphalt layer in between the steel tank bottom and the foundation slab for example;

Such tilting is entirely governed by the stiffness of the OC clay layer under the bearing sand layer and will consequently be ruled on the long run by the time- deformation development of this layer under the tank loading.

References

[1] Van Impe WF, et al. Prediction of the single pile bearing capacity in granular soils out of CPT results, ISOPT I, Proceeding First International symposium on penetration testing (specialty session), 1988.
[2] Van Impe WF, et al. End and shaft bearing capacity of piles evaluated separately out of static pile loading test results, First International Geotechnical seminar Deep Foundations on Bored and Auger Piles, 7-10 juni, Ghent, 1988. pp. 489-498
[3] Robertson PK, Soil classification using the cone penetration test, Canadian Geotechnical Journal 1990;27(1):151-8
[4] Robertson PK, Soil behavior type from the CPT: An update. In International Symposium on Cone Penetration Testing CPT 10, 2010.
[5] Fellenius BH, From strain measurement to load in an instrumented pile, Geotechnical News, 2001.
[6] Fellenius BH, Determining the Resistance Distribution in Piles, Part I: Notes on Shift of No-Load Reading and Residual Load. Geotechnical News Magazine 2002;20(2):35-38
[7] Chin FK, Estimation of the ultimate load of piles from tests not carried to failure, Proceeding 2nd Southeast Asian Conference of Soil Engineering, Singapore, 1970. pp. 81-92